Energies, Stability and Structure Properties of Radicals Derived from Organic Sulfides Containing an Acetyl Group after the •OH Attack: ab Initio and DFT Calculations vs Experiment

Jacqueline Bergès,*,† Nicolas Varmenot,‡ Anthony Scemama,§ Zohreh Abedinzadeh,‡ and Krzysztof Bobrowski‖

LCT, UMR 7616, Université Pierre et Marie Curie, 4 Place Jussieu, 75230 Paris Cedex 5 France, Université René Descartes, 45, rue des Saints Pères, 75006 Paris, France, Laboratoire de Chimie Physique, UMR 8601 CNRS, Université Paris Descartes, 45, rue des Saints Pères, 75006 Paris, France, and Institute of Nuclear Chemistry and Technology, Dorodna 16, 03-195 Warsaw, Poland

Received: December 20, 2007; Revised Manuscript Received: March 14, 2008

The mutual location of the sulfur atom and the acetyl group was found to affect significantly the •OH-induced oxidation mechanism of the organic sulfides containing either an α- or *β*-positioned acetyl group. This phenomenon was reflected in formation of different intermediate products observed in pulse radiolysis experiments (Varmenot et al. *J. Phys. Chem. A.* **2004**, *108*, 6331−6346). In order to obtain a better support for the earlier interpretation of the experimental data, quantum mechanical calculations were performed using a density functional theory method (DFT-B3LYP) and the ab initio method (Møller−Plesset perturbation theory MP2) for optimizations and energy calculations of the parent molecules and radicals and radical cations derived from them. In accordance with experiments, it was found that the α-positioned acetyl group in *S*-ethylthioacetate (SETAc) destabilizes hydroxysulfuranyl radicals and monomeric sulfur radical cations. Instead, formation of stable C-centered radicals of the α-(alkylthio)alkyl-type was found energetically favorable, the $H_3C-{}^{\bullet}CH-S-C(=O)CH_3$ radical, in particular. On the other hand, the *β*-positioned acetyl group in *S*-ethylthioacetone (SETA) does not destabilize hydroxysulfuranyl radicals, monomeric sulfur radical cations, and dimeric sulfur radical cations. Moreover, the α-(alkylthio)alkyl radicals of the type $-S-{}^{\bullet}CH-C(=O)-$ were found to be particularly stabilized. The calculated transition states pointed toward the efficient direct conversion of the hydroxysulfuranyl radicals derived from SETAC and SETA radicals into the respective C-centered radicals. This reaction pathway, important in neutral solutions, is responsible for the absence of the dimeric radical cations of SETAc at low and high concentrations and of the dimeric radical cations of SETA at relatively low concentrations of the solute.

Introduction

The one-electron oxidation of organic sulfides by hydroxyl radicals (•OH) in aqueous solutions has been the subject of many investigations. The oxidation mechanism of simple alkyl sulfides involving •OH radicals is complex, however, it has been very well elaborated.[1–5] A first step is an initial addition of •OH radicals to the sulfur atom resulting in the formation of 2c-3e OH-adducts (hydroxysulfuranyl radicals) (1). The decay of the hydroxysulfuranyl radicals could occur by several reaction pathways (2, 3, 5, and 6) and leads eventually to thermodynamically favored α-(alkylthio)alkyl radicals either directly (5) or via monomeric radical cations, formed preferentially in acidic medium (3 and 4). At high concentrations of the sulfide, the hydroxysulfuranyl radical can be converted into the 2c−3e intermolecularly bonded dimeric radical cation (6). The monomeric radical cation exists also in equilibrium with the 2c−3e intermolecularly bonded dimeric radical cation (7).

$$R_2S + {}^{\bullet}OH \rightarrow [R_2S-OH]^{\bullet} \quad (1)$$

$$[R_2S-OH]^{\bullet} \rightarrow R_2S^{+\bullet} + OH^- \quad (2)$$

$$[R_2S-OH]^{\bullet} + H_3O^+ \rightarrow R_2S^{+\bullet} + 2H_2O \quad (3)$$

$$R_2S^{\bullet+} \rightarrow H^+ + R'^{\bullet}SR \quad \text{with } R' = R(-H) \quad (4)$$

$$[R_2S-OH]^{\bullet} \rightarrow R'^{\bullet}SR + H_2O \quad \text{with } R' = R(-H) \quad (5)$$

$$[R_2S-OH]^{\bullet} + R_2S \rightarrow (R_2S \therefore SR_2)^+ + OH^- \quad (6)$$

$$R_2S^{+\bullet} + R_2S \rightleftharpoons (R_2S \therefore SR_2)^+ \quad (7)$$

The oxidation mechanism of sulfides containing neighboring groups has been found to be even more complex.[1,6–24] This is due to the fact that these neighboring groups generally act by providing electron lone pairs that can stabilize sulfide radical cations ($R_2S^{+\bullet}$) through the overlap of the heteroatoms' doubly occupied p orbitals with the singly occupied p orbital of the sulfur.[2,25,26] The resulting bond is a three-electron bond of the type $2\sigma/1\sigma^*$. Furthermore, $R_2S^{+\bullet}$ and 2c−3e bonded dimeric radical cations can be stabilized or destabilized depending on the presence of electron withdrawing or electron donating adjacent functional groups to the sulfur atom.

In our recent publication,[27] it was demonstrated that the relative location of the sulfur atom and the acetyl group affects

* To whom correspondence should be addressed. Fax: 33 1 44 27 4117. E-mail: jb@lct.jussieu.fr.
† Université Pierre et Marie Curie and Université Paris Descartes.
‡ UMR 8601 CNRS, Université Paris Descartes.
§ Université Pierre et Marie Curie.
‖ Institute of Nuclear Chemistry and Technology.

10.1021/jp711944v CCC: $40.75
Published on Web 07/09/2008

the ultimate course of the sulfide oxidation. For the α-positioned acetyl group in *S*-ethylthioacetate (SETAc) only stable C-centered radicals of the α-alkylthioalkyl-type were observed, consequently indicating that the hydroxysulfuranyl radical and the monomeric sulfur radical cation were destabilized. On the other hand, the *β*-positioned acetyl group in *S*-ethylthioacetone (SETA) does not destabilize radicals. In addition to the stable α-(alkylthio)alkyl radicals of the type −S−•CH−C(═O)−, hydroxysulfuranyl radicals and 2c−3e bonded dimeric radical cations have been observed. In order to obtain better support for our earlier interpretation of the experimental data ab initio and DFT computations were performed for the optimization of energy and structure of the parent molecules and radicals and radical cations derived from them. Possible mechanisms derived from the earlier experimental observations will be discussed in relation with the ab initio and DFT calculations.

Computational Methods

Calculations were performed with Gaussian 98[28] and Gaussian 03[29] packages. For most of the radicals, density functional theory (DFT) was used with the hybrid B3LYP functional and a 6-31G(d) basis set. The accuracy of B3LYP is well-known for the proper description of the localized radical structures.[30,31] The use of this relatively small basis set is justified by the fact that DFT methods are not very basis-set dependent.

However, until now, the answer to which theoretical treatments are adequate for 2c−3e bonds is far from definitive. The multireference computational methods as QCISD(T) or CCSD(T) ones, with very large basis sets, lead to accurate energies and to reliable structures at the same time. As a compromise, for SETAc and SETA molecules whose size is too large to perform energy optimizations with these QCISD(T) or CCSD(T) methods, we chose the MP2/6-31+G(d)[32–37] and B3LYP/6-31G(d) ones. Errors resulting from the basis-set dependence could be significant for the (2c,3e) systems.[38] However, it was shown that 6-31+G(d) basis was accurate for the hydroxysulfuranyl radical.[34,39] Usually, the bond lengths and the binding energies are overestimated within the DFT methods and are underestimated within the MP2 method. However, with the 6-31+G(d) basis set similar binding energies were obtained when MP2 and QCISD(T) and CCSD(T) calculations were performed on the same small molecules.[32,34,36–39]

The transition states, on the reaction pathways from the hydroxysulfuranyl radicals, being not reachable with the MP2 method, we used the B3LYP calculations. We are conscious that B3LYP does not give particularly reliable estimates of transition state energies, but our aim was to roughly compare their relative activation energies and the trends to get the final products.

All structures were fully optimized using the analytical gradient technique. All calculations of radical species, using DFT or MP methods, were carried out within the spin-unrestricted formalism. Spin densities were used to describe localization of unpaired electrons.

Solvation effects in water were accounted for with the COSMO option for the polarized continuum model CPCM with both methods.[40,41] However, only single-point calculations in the gas-phase geometries can be performed with the MP2/6-31+G(d) method because gradients used for optimization are not available in that level. Electrostatic and nonelectrostatic terms are included in the total energy values.

Whereas computational results are probably accurate for gas-phase energies within 2−4 kcal/mol in vacuum, the errors in the liquid phase are much more difficult to estimate.[42] In order to compare the results in both phases the bond dissociation energies (BDE) and reaction energies (Δ*E*) were calculated as the difference between the computed total electronic energies of products (radicals obtained after bond breaking) and reactants (parent molecules). In the solvent the energies of •OH, OH^-, H_2O, and H_3O^+ species were taken into account. Their electronic solvation energies, calculated as the differences between energies in solvent and in vacuum (respectively −4.5, −86.8, −5.9, and −108.1 kcal/mol; see Table 1 entries 23−26) are of the same order of magnitude as solvation free energies[42,43] calculated both with B3LYP (respectively −3.6, −108.2, −3.0, and −105.5 kcal/mol).[42]

Results

Molecules of SETAc and SETA and radicals derived from them were studied together in order to check the influence of the α and *β* positioned acetyl group on the oxidation reaction pathways induced by •OH radicals.

Conformational Analysis of SETAc and SETA Molecules. A complete conformational analysis of model compounds (SETAc and SETA) was performed with the B3LYP method. Several stable conformations were obtained. However, only the two most stable conformations for SETAc (Figure 1, structure **a1**) and SETA (Figure 1, structure **b1**) are displayed. Their energies are listed in Table 1 (entries 6 and 15) for SETAc and SETA, respectively. Moreover, the MP2 method was also applied for the optimization of energy for two most stable conformers.

Hydroxysulfuranyl Radicals. Hydroxysulfuranyl radicals are neutral species resulting from the addition of a hydroxyl radical to a sulfur atom and theoretical calculations performed on them[32,34,39,42–48] point out the methodological difficulties to treat that kind of radicals. In fact, the S−O bond is not easy to characterize topologically as a two center three-electron (2c−3e) bonds. It could have in some cases a character purely electrostatic, depending of the substitutions. Therefore, qualitative and quantitative criteria, defined from the topological analysis of the electron localization function (ELF), were proposed. For instance, in the OH-adduct in dimethyl sulfide (DMS), the S−O bond exhibits features of a weak covalent bond because of a quasi-uniform spin delocalization between sulfur and oxygen atoms.[34]

However, for the hydroxysulfuranyl radicals formed in SETAc and SETA, we have to take into account the following two features: (i) S−O bonds are unsymmetrical, not only because of two different heteroatoms forming the bond but also because of the different substituents linked to these atoms. (ii) These three-electron bonded adducts are not easily characterized and although they have been detected, their structural features cannot be probed.

The stability of hydroxysulfuranyl radicals derived from SETAc and SETA was compared with that of the hydroxysulfuranyl radical derived from DMS. The bond dissociation energy is defined as BDE = *E*(parent molecule) + *E*(•OH) − *E*(OH-adduct). The results, including energies of radicals (Table 1, entries 2, 7, and 16), BDEs (Table 2, entries 1, 3, and 8), selected bond lengths and spin densities on sulfur, carbon, and oxygen atoms (Table 3 entries 1, 5, and 11) are presented for DMS, SETAc, and SETA, respectively.

Dimethylsulfide (DMS). The hydroxysulfuranyl radical derived from DMS was found to be stable in vacuum and in water. This is in agreement with experimental observations[4,18] and with the first theoretical calculations performed on this species at the MP2/6-31+G(2d) level.[39] The calculated BDE is equal to

TABLE 1: Energies (in a.u.) of Selected Optimized Structures of Organic Sulfides and Optimized Structures of Radicals Derived from Them [a] Calculated with the MP2/6-31+G(d) Method [b] Calculated with the B3LYP/6-31G(d) Method

entry	entity	energy (a.u.) (in vacuum)	energy (a.u.) (in water)
1	$(CH_3)_2S$	−477.12588[a]−478.01381[b]	−477.12816[a]−478.01569[b]
2	$(CH_3)_2S^{\bullet}OH$	−552.67099[a]	−552.67156[a]
3	$(CH_3)_2S^{\bullet+}$	−476.82053[a]−477.69910[b]	−476.90684[a]−477.78486[b]
4	$[(CH_3)_2S\therefore S(CH_3)_2]^+$	−953.99547[a]−955.76475[b]	−954.06294[a]−955.81587[b]
5	$H_2C^{\bullet}-S-CH_3$	−477.35164[b]	
6	$CH_3-CO-S-CH_2-CH_3$	−629.34956[a]−630.66897[b]	−629.35330[a]−630.67187[b]
7	$CH_3-CO-S^{\bullet}OH-CH_2-CH_3$	not converged[a]−706.40618[b]	not converged[a]−706.41258[b]
8	$CH_3-CO-S^{\bullet+}-CH_2-CH_3$	−630.34210[b]	−630.41998[b]
9	$CH_3-CO-S-CH_3$	−590.17987[a]	−590.18358[a]
10	$CH_3-CO-S^{\bullet+}-CH_3$	−589.85117[a]	−589.93365[a]
11	$[CH_3(CH_3-CO)-S\therefore S-(CO-CH_3)CH_3]^+$ $[C_2H_5(CH_3-CO)-S\therefore S-(CO-CH_3)C_2H_5]^+$	−1180.07427[a]−1261.04061[b]	−1180.13724[a]
12	$H_2C^{\bullet}-CO-S-CH_2-CH_3$	−630.00702[b]	−630.01035[b]
13	$H_3C-CO-S-{}^{\bullet}CH-CH_3$	−630.00503[b]	−630.00857[b]
14	$H_3C-CO-S-CH-{}^{\bullet}CH_2$	−629.99844[b]	−630.00222[b]
15	$CH_3-CO-CH_2-S-CH_2-CH_3$	−668.50462[a]−669.96863[b]	−668.51103[a]−669.97373[b]
16	$CH_3-CO-CH_2-S^{\bullet}OH-CH_2-CH_3$	−744.04492[a]−745.70862[b]	−744.05006[a]−745.71710[b]
17	$CH_3-CO-CH_2-S^{\bullet+}-CH_2-CH_3$	−669.669316[b]	−669.74940[b]
18	$[C_2H_5(CH_3-CO)CH_2-S\therefore SCH_2-(CO-CH_3)C_2H_5]^+$	−1339.67975[b]	
19	$H_2C^{\bullet}-CO-CH_2-S-CH_2-CH_3$	−669.30873[b]	−669.31418[b]
20	$H_3C-CO-{}^{\bullet}CH-S-CH_2-CH_3$	−669.32967[b]	−669.33466[b]
21	$H_3C-CO-CH_2-S-{}^{\bullet}CH-CH_3$	−669.30891[b]	−669.31445
22	$H_3C-CO-CH_2-S-CH_2-{}^{\bullet}CH_2$	−669.29896[b]	−669.30443[b]
23	$^{\bullet}OH$	−75.53133[a]−75.72345[b]	−75.54056[a]−75.73060[b]
24	OH^-	−75.72077[b]	−75.85918[b]
25	H_2O	−76.40895[b]	−76.41837[b]
26	H_3O^+	−76.68908[b]	−76.86129[b]

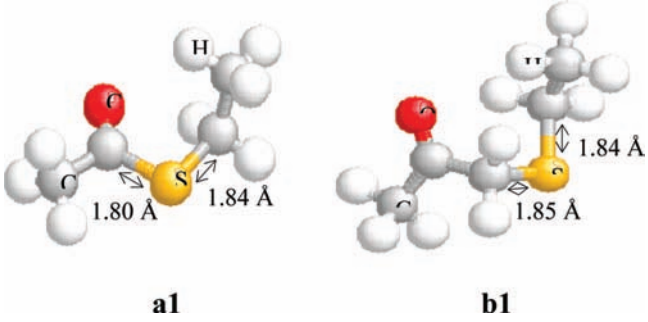

Figure 1. Structures of the most stable conformations of neutral molecules: SETAC (**a1**) and SETA (**b1**).

8.6 kcal mol^{-1} (Table 2, entry 1, left). However, the aqueous environment has a strong destabilizing effect since the BDE decreases to 1.8 kcal mol^{-1} (Table 2, entry 1, right). As it was noted previously for the nonsymmetrical S−O bond, the spin density is quite equally distributed between both atoms, even in water when the bond strength decreased (Table 3, entry 1).

S-Ethylthioacetate (SETAc). As far as the stability of the hydroxysulfuranyl radical is concerned, two different results were obtained, depending on the calculation method used. With the MP2/6-31+G(d) method, the OH-adduct of SETAc did not show any stability, irrespective of any starting conformation and environment (Table 2, entry 3). For instance, no stabilization by the hydrogen-bond between OH and the carbonyl group >C═O was found. This result of calculations for the OH-adduct differs from the result obtained for the OH-adduct of DMS with the same method (vide supra). On the other hand, with the B3LYP method which is known to overestimate stabilization energy, the OH-adduct of SETAc was found to be stable (Table 2, entry 5).

S-Ethylthioacetone (SETA). In SETA, where the sulfur atom is separated from the acetyl group by a methylene group, a stable OH-adduct can be obtained as in DMS, using both methods. Only the most stable conformation is shown in Figure 2 since similar energies, local geometry around sulfur atom, and spin density distributions were found for all other conformers of the OH-adduct in SETA. In the most stable conformation, the hydroxyl group remains perpendicularly located to the plane including a sulfur atom and a carbonyl group (SC═O) in a T-shaped sulfur geometry (Figure 2).

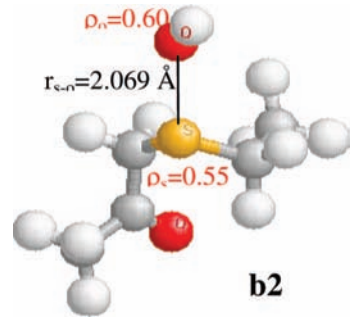

Figure 2. Geometrical structure of the hydroxysulfuranyl radical in SETA.

For instance, a cyclic conformer of the OH-adduct possessing an intramolecular hydrogen bonding involving the carbonyl oxygen was found unfavorable by 15 kcal mol^{-1}. The calculated BDE from the MP2 method for the T-shaped OH-adduct is equal to 5.6 kcal mol^{-1} (Table 2, entry 8) which is of the same order of the magnitude as that for the OH-adduct in DMS (Table 2, entry 1). Again, the aqueous medium has a strong destabilizing effect since the computed BDE decreased to −1 kcal mol^{-1} (Table 2, entry 8). The calculated BDE from the B3LYP method (Table 2 entry 8) are larger as was expected.

It has to be stressed that the OH-adduct of SETA is characterized by a similar geometry and energy to those of the OH-adduct of DMS. The SO bond length is again rather short, in the range of ∼2.07 Å, and the spin density is also equally

TABLE 2: Bond Dissociation Energies (BDE) of Radical Derived from DMS, SETAc, and SETA [a] Calculated with the MP2/6-31+G(d) Method, [b] Calculated with the B3LYP/6-31G(d) Method[a]

entry	entity	BDE (kcal mol^{-1}) (in vacuum)	BDE (kcal mol^{-1}) (in water)
1	$(CH_3)_2S^{\bullet}OH$	8.6[a]	1.8[a]
2	$[(CH_3)_2S\therefore S(CH_3)_2]^+$	30.8[a]	17.5[a]
		32.5[b]	19.0[b]
3	$CH_3-CO-S^{\bullet}OH-CH_2-CH_3$	not converged,[a] 8.6[b]	not converged,[a] 6.2[b]
4	$[CH_3(CH_3-CO)-S\therefore S-(CO-CH_3)CH_3]^+$	27.1[a]	12.6[a]
	$[C_2H_5(CH_3-CO)-S\therefore S-(CO-CH_3)C_2\ H_5]^+$	19.2[b]	
5	$H_2C^{\bullet}-CO-S-CH_2-CH_3$	101.5[b]	102.7[b]
6	$H_3C-CO-S-{}^{\bullet}CH-CH_3$	102.7[b]	103.8[b]
7	$H_3C-CO-S-CH_2-{}^{\bullet}CH_2$	106.8[b]	107.8[b]
8	$CH_3-CO-CH_2-S^{\bullet}OH-CH_2-CH_3$	5.6[a]	−1.0[a]
9	$[C_2H_5(CH_3-CO)CH_2-S\therefore SCH_2-(CO-CH_3)C_2\ H_5]^+$	30.5[b]	
10	$H_2C^{\bullet}-CO-CH_2-S-CH_2-CH_3$	100.2[b]	101.4[b]
11	$H_3C-CO-{}^{\bullet}CH-S-CH_2-CH_3$	87.0[b]	88.6[b]
12	$H_3C-CO-CH_2-S-{}^{\bullet}CH-CH_3$	100.1[b]	101.3[b]
13	$H_3C-CO-CH_2-S-CH_2-{}^{\bullet}CH_2$	106.3[b]	107.6[b]

[a] BDE are defined as follows: E(parent molecule) + E($^{\bullet}$OH) − E(OH-adduct) for entities 1, 3 and 8; [E(parent molecule) + E(monomer radical cation) − E(dimeric radical cation) for entities 2 and 4; and E(radical alkyle) + E($^{\bullet}$H) − E(parent molecule) for entities 5−7 and 10−13.

distributed (Table 3, entry 11) between the sulfur and oxygen atoms although the groups linked to both atoms are different.

The influence of solvent and substituents on the energies of OH-adducts discerned from an analysis of results shown in Table 2 and 3 leading to the following conclusions:

(i) The difference between the bond dissociation energies of the OH-adducts of dimethylsulfide (DMS) and *S*-ethylthioacetone (SETA) in vacuum reflects the influence of the electronic effects of the substituents. In DMS, there are only weakly electron releasing substituents (two methyl groups). On the other hand, in SETA there is a balance between electron releasing (an ethyl group) and electron withdrawing (an acetyl group) effects.

(ii) When electronic factors are favorable, the BDE of the OH-adduct dramatically decreases in aqueous solutions to 1.8 kcal mol^{-1} for DMS and becomes even negative (−1 kcal mol^{-1}) for SETA (Table 2, entries 1 and 8). These small bond dissociation energies are in agreement with the very short lifetimes of OH-adducts that are experimentally observed in aqueous solutions.

Monomeric Sulfur Radical Cations ($R_2S^{+\bullet}$). Since the unpaired electron is localized in the monomeric sulfur radical cation, both MP2 and B3LYP methods gave similar results. In order to study the formation of the monomeric radical cations, first the adiabatic ionization potentials (IP = energy (parent molecule) − energy (radical cation)) of DMS, SETAc, and SETA, and second, the energies of the respective reactions (vide infra) without and with the involvement of protons, both were calculated in vacuum and water.

Comparison of the ionization potentials (IP) of SETAc (8.89 eV), DMS (8.56 eV), and SETA (8.14 eV) calculated in vacuum points out that the presence of the carbonyl group adjacent to the sulfur atom makes ionization of SETAc less favorable. On the other hand, separation of the sulfur atom and the carbonyl group by the methylene group makes ionization of SETA more favorable. The same conclusion applies for the ionization of SETAc (IP = 6.85 eV), DMS (IP = 6.28 eV), and SETA (IP = 6.10 eV) in water.

Monomeric sulfur radical cations ($R_2S^{+\bullet}$) can be formed with an involvement of the $^{\bullet}$OH radical via a sequence of reactions (1) and (2). For the overall process $R_2S + {}^{\bullet}OH \rightarrow R_2S^{+\bullet} + OH^-$ we can define the energy as $\Delta E' = E(R_2S^{+\bullet}) + E(OH^-) - E(R_2S) - E({}^{\bullet}OH)$. In order to mimic reactions occurring in acidic medium, reaction 2 has to be replaced by (3) and the overall process leading to $R_2S^{+\bullet}$ is described as $R_2S + {}^{\bullet}OH + H_3O^+ \rightarrow R_2S^{+\bullet} + 2H_2O$. In this case, the energy of the overall process is $\Delta E'' = E(R_2S^{+\bullet}) + 2E(H_2O) - E(R_2S) - E({}^{\bullet}OH) - E(H_3O^+)$. It must be emphasized that modeling of proton in water by H_3O^+ is a crude approximation.

Dimethyl Sulfide (DMS). Energy calculations in vacuum reveal that the formation of $(CH_3)_2S^{+\bullet}$ is strongly unfavorable: $\Delta E' = 199.2$ kcal mol^{-1} and $\Delta E'' = 41.1$ kcal mol^{-1}. Calculated energies in water ($\Delta E'$ and $\Delta E''$) indicate that formation of $(CH_3)_2S^{+\bullet}$ without the involvement of protons is again strongly unfavorable by 150.6 kcal mol^{-1}. However, its formation becomes slightly favorable by 0.14 kcal mol^{-1} when protons are involved.

S-Ethylthioacetate (SETAc). Similar energy calculations (for $\Delta E'$ and $\Delta E''$) have been performed for SETAc (Table 4, entry 1). It is noteworthy that formation of the monomeric radical cation derived from SETAc, $H_3C-C(=O)S^{+\bullet}-CH_2-CH_3$, in vacuum and in water is unfavorable without and with the involvement of protons. In water, both processes are energetically unfavorable by 170.6 and 10.8 kcal mol^{-1}, respectively (Table 4, entry 1).

Furthermore, the monomeric radical cation ($R_2S^{+\bullet}$) of SETAc can adopt two different conformations. The first conformation is close to the conformation of a parent molecule with SC bonds remaining around 1.8 Å (Table 3, entry 6, bottom). The second conformation (Figure 3, structure **a3**) is slightly more stable. However, there is a substantial stretching up to 2.09 Å of the SC bond (involving carbon atom in the acetyl group) (Table 3, entry 6, top). The bond length is much too long to form a covalent bond, and consequently, this bond can be easily broken.

S-Ethylthioacetone (SETA). Energy calculations (for $\Delta E'$ and $\Delta E''$) have been performed for SETA (Table 4, entry 5). In water, formation of the monomeric sulfur radical cation derived from SETA, $H_3C(=O)CH_2S^{+\bullet}CH_2CH_3$, without the involvement of protons is again strongly energetically unfavorable by 155 kcal mol^{-1}. However, its formation becomes energetically favorable only by 4.9 kcal mol^{-1} when protons are involved.

Contrary to what was found in SETAc, the SC bond lengths remain almost identical to those in the parent molecule in all possible conformations (Figure 3, structure **b3**). On the other

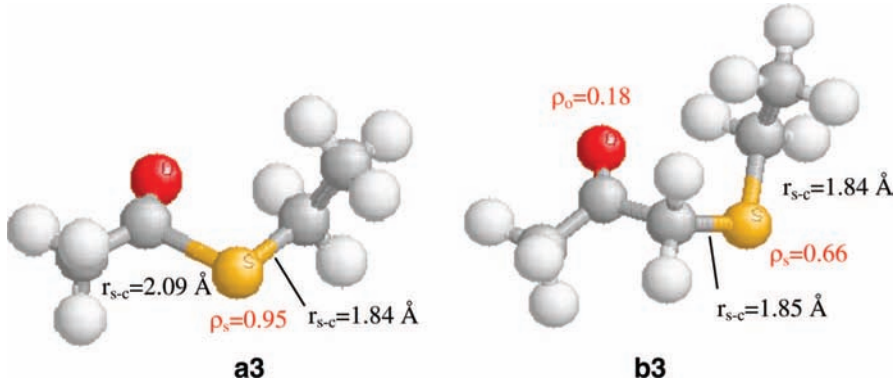

Figure 3. Geometrical structures of the monomeric sulfur radical cations in SETAc (**a3**) and SETA (**b3**).

hand, the spin density is not uniformly distributed between the sulfur atom, $\rho_S = 0.64-0.66$, and the oxygen atom of the carbonyl group, $\rho_O = 0.20-0.18$, resulting from folding of the cation.

It has to be stressed that formation of the monomeric sulfur radical cation derived from SETA is characterized by similar energetic features as is the formation of the monomeric sulfur radical cation derived from DMS. Without the involvement of protons, formation of both radical cations is strongly unfavorable energetically in the gas phase and in water. On the other hand, when protons are involved, formation of both monomeric radical cations is energetically unfavorable only in the gas-phase.

Dimeric Radical Cations $(R_2S\therefore SR_2)^{\bullet+}$. Dimeric radical cations $(R_2S\therefore SR_2)^{\bullet+}$ can be formed either via direct interaction of a monomeric radical cation ($R_2S^{+\bullet}$) with a parent R_2S molecule (reaction 7) or by replacement of the OH functionality by R_2S in the OH-adduct (reaction 6). For the first process, we can define BDE for the dimeric radical cation as BDE = $E(R_2S^{+\bullet}) + E(R_2S) - E((R_2S\therefore SR_2)^{\bullet+})$. For the second process (reaction 6), we can define the energy as $\Delta E' = E((R_2S\therefore SR_2)^{\bullet+}) + E(OH^-) - E(R_2S\ \therefore OH) - E(R_2S)$.

Calculations were performed on DMS and *S*-methyl thioacetate (SMTAc) using MP2/6-31+G(d) method. Substitution of the ethyl group by the methyl group was justified by the size of the dimeric sulfur radical cation entity. Furthermore, we performed geometry optimization calculations with B3LYP/6-31G(d) method on the dimeric radical cations of DMS, SETAc, and SETA in vacuum and in solvent for DMS.

Dimethyl Sulfide (DMS), S-Methylthioacetate (SMTAc), and S-Ethylthioacetate (SETAc). Comparison between the MP2/6-31+G(d) and B3LYP/6-31G(d) results shows that in the case of symmetrical 2c−3e bonds in cations the trends are similar. In spite of the fact that formation of the monomeric sulfur radical cations is strongly unfavorable both for DMS and SETAc, dimerization is easy in vacuum: −30.8 kcal mol^{-1} with MP2 and −32.5 kcal/mol with B3LYP (Table 2, entry 2) for DMS, and −27.18 kcal mol^{-1} for SMTAc with MP2 and −19.2 kcal mol^{-1} for SETAc with B3LYP (Table 2, entry 4) in the presence of their respective native molecules. These dimerizations remain also very favorable in water: −17.5 kcal mol^{-1} (Table 2, entry 2) for DMS and −12.6 kcal mol^{-1} (Table 2, entry 4) for SMTAc.

The decrease in the formation energy calculated for the dimeric sulfur radical cations of SMTAc and of SETAc compared to that of the dimeric sulfur radical cations of DMS is in line with a concomitant slight lengthening of the SS bond (2.787 Å for DMS versus 2.856 Å for SMTAc and 2.943 Å for SETAc) (Table 3 entries 3 and 7). Futhermore for the dimeric radical cation of SETAc, steric hindrances were observed when the ethyl group replaces the methyl one. One can note that the length of the SC bond between the sulfur and the carbonyl group is close to that of the analogous S−C bond in the monomeric radical cation (r_{S-C} = 2.1 for SMTAc and 1.9 Å for SETAc; Table 3, entry 7).

As it was expected for symmetrical dimeric radical cations the spin densities are almost equally distributed between the two sulfur atoms in the dimeric radical cations derived from DMS and SMTAc (Table 3, entries 3 and 7). For the dimeric radical cation of SETAc, the spin densities reflect the unsymmetrical structure (0.42 and 0.52, Table 3 entry 7).

S-Ethylthioacetone (SETA). Concerning the SETA molecule, calculations with MP2/6-31+G(d) are not feasible because of the size of the molecule. However, when comparing the results obtained earlier for the OH-adduct and the monomeric sulfur radical cation in DMS and in SETA, one can conclude that the presence of methylene group adjacent to the sulfur atom in SETA could lead only to minor changes. Therefore, it is reasonable to extrapolate and to assume that the dimerization energy will be of the same order of magnitude as the dimerization energy calculated for DMS i.e. ∼−30 kcal mol^{-1} in vacuum and ∼−17 kcal mol^{-1} in water (vide supra). This was verified with B3LYP/6-31G(d) for SETA in vacuum: −30.5 kcal mol^{-1} (Table 2 entry 9). The SS bond is slightly longer, 3.007 Å, the spin densities are almost the same on both sulfur atoms (0.46−49 Table 3 entry 13).

C-Centered Radicals. Since the electron is localized in C-centered radicals, as in the monomeric sulfur radical cations, the B3LYP method was used for calculations of their energies, BDEs, and formation energies. The BDE values give an insight on the bond strengths with respect to homolytic cleavage of the CH bonds.

The following two reaction pathways were considered for the formation of C-centered radicals: first, hydrogen atom abstraction by hydroxyl radical (reaction 8):

$$R_2S + {}^{\bullet}OH \rightarrow RS^{\bullet}R' + H_2O \text{ with } R' = R(-H) \qquad (8)$$

and second, water-assisted deprotonation of the monomeric sulfur radical cation (reaction 9):

$$R_2S^{+\bullet} + H_2O \rightarrow RS^{\bullet}R' + H_3O^+ \text{ with } R' = R(-H) \qquad (9)$$

For the overall processes described by reactions 8 and 9, we can define the respective energies as $\Delta E' = E(RS^{\bullet}R') + E(H_2O) - E(R_2S) - E({}^{\bullet}OH)$ and $\Delta E'' = E(RS^{\bullet}R') + E(H_3O^+) - E(R_2S^{+\bullet}) - E(H_2O)$.

In order to complete the energetic approach, the energy levels along the possible reaction pathways described by reactions 1 and 5 (vide supra) in SETAc and SETA were calculated. As it

TABLE 3: Selected Bond Lengths and Spin Densities in Optimized Solvated Radicals Derived from DMS, SETAc, and SETA [a] Calculated with the MP2/6-31+G(d) Method, [b] Calculated with the B3LYP/6-31G(d) Method, [c] Conformation 1, and [d] Conformation 2

entry	entity	bond length (Å)	spin density (ρ)
1	$(CH_3)_2S^{\bullet}-OH$	S−O, 2.0676[a]	S, 0.53[a] O, 0.61[a]
2	$(CH_3)_2S^{\bullet+}$	C−S, 1.792[b]	S, 0.92[b]
3	$[(CH_3)_2S\therefore S(CH_3)_2]^+$	S−S, 2.787[a]	S, 0.54[a]
4	$H_2C^{\bullet}-S-CH_3$	(2H)C−S, 1.728[b] (3H)C−S, 1.828[b]	C, 0.90[b] S, 0.16[b]
5	$CH_3-CO-S^{\bullet}(OH)-CH_2-CH_3$	not converged[a] S−O, 2.248[b]	not converged[a]
6	$CH_3-CO-S^{\bullet+}-CH_2-CH_3$	(O)C−S, 1.81[b,c] (O)C−S, 2.09[b,d] (H)C−S, 1.84[b,cn]	S, 0.87[b,c] O, 0.20[b,c] S, 0.95[b,d]
7	$[CH_3(CH_3-CO)-S\therefore S-(CO-CH_3)CH_3]^+$	S−S, 2.856[a] (O)C−S, 2.107[a]	S, 0.58[a]
	$[C_2H_5(CH_3-CO)-S\therefore S-(CO-CH_3)C_2\ H_5]^+$	S−S, 2.943[b] (O)C−S, 1.908[b]	S, 0.52[a] S, 0.42[a]
8	$CH_3-CO-S-{}^{\bullet}CH-CH_3$	(O)C−S, 1.83[b] (H)C−S, 1.74[b]	C, 0.95[b]
9	$^{\bullet}CH_2-CO-S-CH_2-CH_3$	(2H)C−C(O), 1.441[b] (O)C−S, 1.814[b] (2H)C−S, 1.537[b]	C, 0.92[b] O, 0.19[b] (O)C, −0.10[b]
10	$CH_3-CO-S-CH_2-{}^{\bullet}CH_2$	(O)C−S, 1.805[b] (2H)C−S, 1.890[b] (2H)C−C(2H), 1.471[b]	C, 1.03[b] S, 0.13[b] (2H)C, −0.09[b]
11	$CH_3-CO-CH_2-S^{\bullet}(OH)-CH_2-CH_3$	S−O, 2.0685[a] 2.397[b]	S, 0.55[a] O, 0.60[a]
12	$CH_3-CO-CH_2-S^{\bullet+}-CH_2-CH_3$	C−S, 1.85[b] S−C, 1.84[b]	S, 0.66[b] O, 0.18[b]
13	$[C_2H_5(CH_3-CO)CH_2-S\therefore SCH_2-(CO-CH_3)C_2\ H_5]^+$	S−S, 3.007[b]	S, 0.49[b] S, 0.46[a]
14	$CH_3-CO-{}^{\bullet}CH-S-CH_2-CH_3$	(O)C−C, 1.44[b] (H)C−S, 1.74[b] S−C(2H), 1.85[b]	S, 0.23[b] O, 0.23[b] C, 0.57[b]
15	$^{\bullet}CH_2-CO-CH_2-S-CH_2-CH_3$	(2H)C−C(O), 1.435[b] (O)C−C(2H), 1.530[b] (2H)C−S, 1.842[b]	C, 0.88[b] O, 0.32[b] (O)C, −0.14[b]
16	$CH_3-CO-CH_2-S-{}^{\bullet}CH-CH_3$	(2H)C−S, 1.846[b] (H)C−S, 1.740[b] (H)C−C(3H), 1.495[b]	C, 0.90[b] S, 0.17[b]
17	$CH_3-CO-CH_2-S-CH_2-{}^{\bullet}CH_2$	(2H)C−S, 1.845[b] S−C(2H), 1.880[b] (2H)C−C(2H), 1.476[b]	C, 1.04[b]

TABLE 4: Reaction Energies Related to the Formation of Radicals and Radical Cations Derived from Thioethers [a] Energies (kcal mol^{-1}) Calculated with the B3LYP/6-31G(d) Method; [b] Energies (kcal mol^{-1}) Calculated for the Overall Process Described by Reactions (1) and (2); [c] Energies (kcal mol^{-1}) Calculated for the Overall Process Described by Reactions (1) and (3); [d] Energies (kcal mol^{-1}) Calculated for the Overall Process Described by Reaction 8; [e] Energies (kcal mol^{-1}) Calculated for the Overall Process Described by Reaction 9

entry	entity	$\Delta E'$[a] (in vacuum)	$\Delta E''$[a] (in vacuum)	$\Delta E'$[a] (in water)	$\Delta E''$[a] (in water)
1	$H_3C-CO-S^{\bullet+}-CH_2-CH_3$	+206.8[b]	+48.7[c]	+170.6[b]	+10.8[c]
2	$H_2C^{\bullet}-CO-S-CH_2-CH_3$	−14.8[d]	+34.5[e]	−16.3[d]	−23.1[e]
3	$H_3C-CO-S-{}^{\bullet}CH-CH_3$	−13.5[d]	+35.7[e]	−15.2[d]	−22.0[e]
4	$H_3C-CO-S-CH-{}^{\bullet}CH_2$	−9.4[d]	+39.9[e]	−11.2[d]	−18.0[e]
5	$H_3C-CO-CH_2-S^{\bullet+}-CH_2-CH_3$	+189.5[d]	+31.4[e]	+155.0[d]	−4.9[e]
6	$H_2C^{\bullet}-CO-CH_2-S-CH_2-CH_3$	−16.1[b]	+50.5[c]	−17.6[b]	−7.1[c]
7	$H_3C-CO-{}^{\bullet}CH-S-CH_2-CH_3$	−43.6[d]	+37.3[e]	−41.2[d]	−19.9[e]
8	$H_3C-CO-CH_2-S-{}^{\bullet}CH-CH_3$	−16.2[d]	+50.4[e]	−17.8[d]	−7.2[e]
9	$H_3C-CO-CH_2-S-CH_2-{}^{\bullet}CH_2$	−9.9[d]	+56.6[e]	−11.5[d]	−9.4[e]

has been pointed out earlier, the optimizations of the structures and transition states, in particular, are not possible with the MP2 method. Therefore, the B3LYP method was used, keeping in mind its limitation, connected with the overestimation of stabilization energy of the OH-adduct.

S-Ethylthioacetate (SETAc). The energies, BDEs, and formation energies of three C-centered radicals which can be formed by homolytic abstraction of hydrogen atoms from the methylene group and two terminal methyl groups were calculated.

First, it was shown that these three C-centered radicals are stable *in vacuum* and in water (Table 1, entries 12−14). Second, the two C-centered radicals $H_3C-CH_2-S-{}^{\bullet}C(=O)-{}^{\bullet}CH_2$ and $H_3C-{}^{\bullet}CH-S-{}^{\bullet}C(=O)CH_3$ (Figure 4, structure **a4**) show similarly large stability in vacuum and water. Both of them are

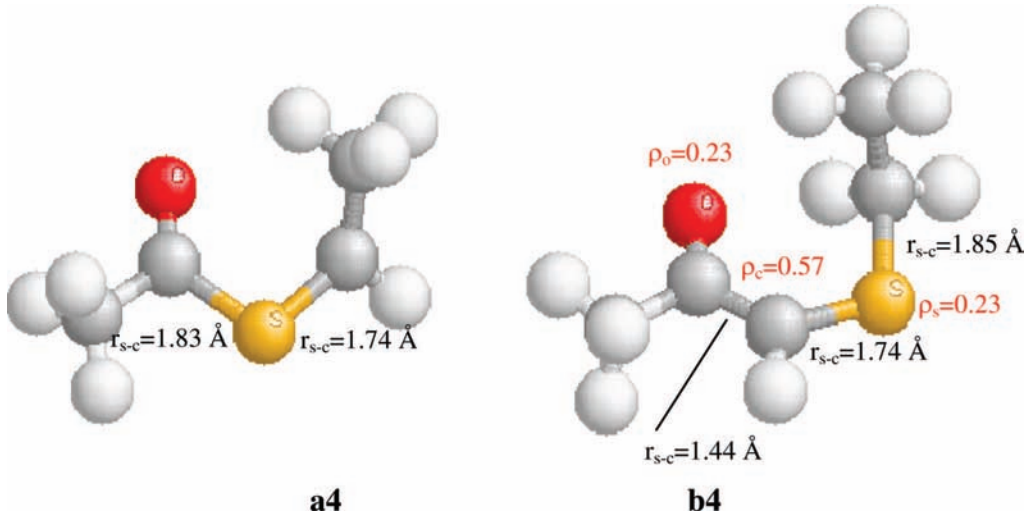

Figure 4. Geometrical structures of the C-centered radicals in SETAc (**a4**) and SETA (**b4**).

characterized by similar BDEs (Table 2, entries 5 and 6). The third one, $H_2C^{\bullet}-CH_2-S-^{\bullet}C(=O)-CH_3$, is characterized by the slightly larger BDE by about 4 to 5 kcal, and thus by the slightly smaller stability (Table 2, entry 7). The BDEs for all three radicals in vacuum and in water differ only by about 1 kcal mol^{-1} (Table 2, entries 5−7).

A detailed analysis of results summarized in Table 1 and 2 leads to the following conclusions with respect to the influence of solvent and substituents on the stability of C-centered radicals:

(i) The most stable C-centered radicals are those with an adjacent electron-withdrawing carbonyl group or an electron donating thioether group next to the radical site.

(ii) The stability of the C-centered radicals does not depend on the environment, i.e. whether they exist in vacuum or in water.

Reaction energies ($\Delta E'$) calculated in vacuum and in water indicate that the formation of C-centered radicals via direct H-atom abstraction by the $^{\bullet}OH$ radicals is strongly favorable, in particular, for the two C-centered radicals $H_3C-CH_2-S-C(=O)-^{\bullet}CH_2$ and $H_3C-^{\bullet}CH-S-C(=O)CH_3$ ($\Delta E' = -14.8$ and -13.5 kcal mol^{-1} in vacuum and $\Delta E' = -16.3$ and -15.2 kcal mol^{-1} in water, respectively; Table 4 entries 2 and 3). The formation of the third radical $H_2C^{\bullet}-CH_2-S-C(=O)-CH_3$ is slightly less energetically favorable ($\Delta E' = -9.4$ kcal mol^{-1} in vacuum and -11.2 kcal mol^{-1} in water; Table 4, entry 4). These values follow perfectly the trend found for the BDEs.

In the case where deprotonation of the monomeric sulfur radical cation assisted by water was considered, the reaction energies ($\Delta E''$) calculated in vacuum indicated that the formation of C-centered radicals is strongly unfavorable (Table 4, entries 2−4). On the other hand, the reaction energies ($\Delta E''$) calculated in water show that the deprotonation process is even more favorable by ~7 kcal mol^{-1} than a direct hydrogen abstraction by $^{\bullet}OH$ radicals (Table 4, entries 2−4). The reaction energies ($\Delta E'$) calculated for the formation of two C-centered radicals $H_3C-CH_2-S-C(=O)-^{\bullet}CH_2$ and $H_3C-^{\bullet}CH-S-C(=O)CH_3$ with $\Delta E' = -23.1$ and -22.0 kcal mol^{-1}, respectively (Table 4, entries 2 and 3) confirm again that the process is energetically favorable. The formation of the third radical $H_2C^{\bullet}-CH_2-S-C(=O)-CH_3$ is slightly less energetically favorable ($\Delta E'' = -18.0$.kcal mol^{-1}; Table 4, entry 4).

To compare the ease of hydrogen abstraction from the various carbon atoms we calculated the transition states geometries and energies using B3LYP. We are conscious that errors are inherent to that type of DFT calculations (vide supra in computational details), but our aim was to get the relative values of the activation energies. The results (see Table 1 entry 7) have revealed some stability of the OH-adduct in SETAc, this intermediate (though very short-lived) can be a precursor for the C-centered radicals. For this purpose energies of the respective transition states (SETAc-TS) were calculated (Table 5, entries 1−2).

TABLE 5: Energies of Transition States along Reaction 5 Pathway for SETAc and SETA [a] in Vacuum, [b] in Water, and [c] Calculated within B3LYP/6-31G(d) Method

	$E^{a,c}$ in a.u.	$(E + ZPE)^{a,c}$ in a.u.	$E^{b,c}$ in a.u.
SETAc-TS1	−706.3627	−706.2407	−706.3677
SETAc-TS2	−706.3843	−706.2637	−706.3919
SETA-TS1	−745.6822	−745.5286	−745.6894
SETA-TS2	−745.6872	−745.5358	−745.6955
SETA-TS3	−745.6912	−745.5418	−745.7036

It was found that the activation energies for the formation of the two transition states SETAc-TS1 (Figure 5, structure **a5**) and SETAc-TS2 are in a very narrow range (10.2−10.4 kcal mol^{-1}). The SETAc-TS1 and SETAc-TS2 convert into the two C-centered radicals characterized by similar stabilization energies (Figure 5).

The activation energy for the formation of the transition state SETAc-TS3 (approach of the $^{\bullet}OH$ radical to the acetyl group) is larger (24 kcal mol^{-1}) and the transition state undergoes dissociation giving acetic acid and an ethylthiyl radical. With this transition state being high in energy, other processes could occur like hydrogen abstraction from the acetyl group. The corresponding C-centered radical, $H_3C-CH_2-S-^{\bullet}C(=O)-^{\bullet}CH_2$, was found to be stable (Table 2, entry 5), but the pathway could not be characterized.

S-Ethylthioacetone (SETA). Similar to the case for SETAc, the energies, BDEs, and formation energies were calculated for the four C-centered radicals which can be formed by homolytic abstraction of hydrogen atoms from the two methylene groups adjacent to the sulfur and two terminal methyl groups.

It was shown that these four C-centered radicals are stable in vacuum and in water (Table 1, entries 19−22). However, one of them, $H_3C-C(=O)-^{\bullet}CH-S-CH_2-CH_3$ (Figure 4, structure **b4**) shows much greater stability in vacuum and water. It is characterized by a much smaller BDE (Table 2, entry 11) as compared to the remaining three radicals (Table 2, entries

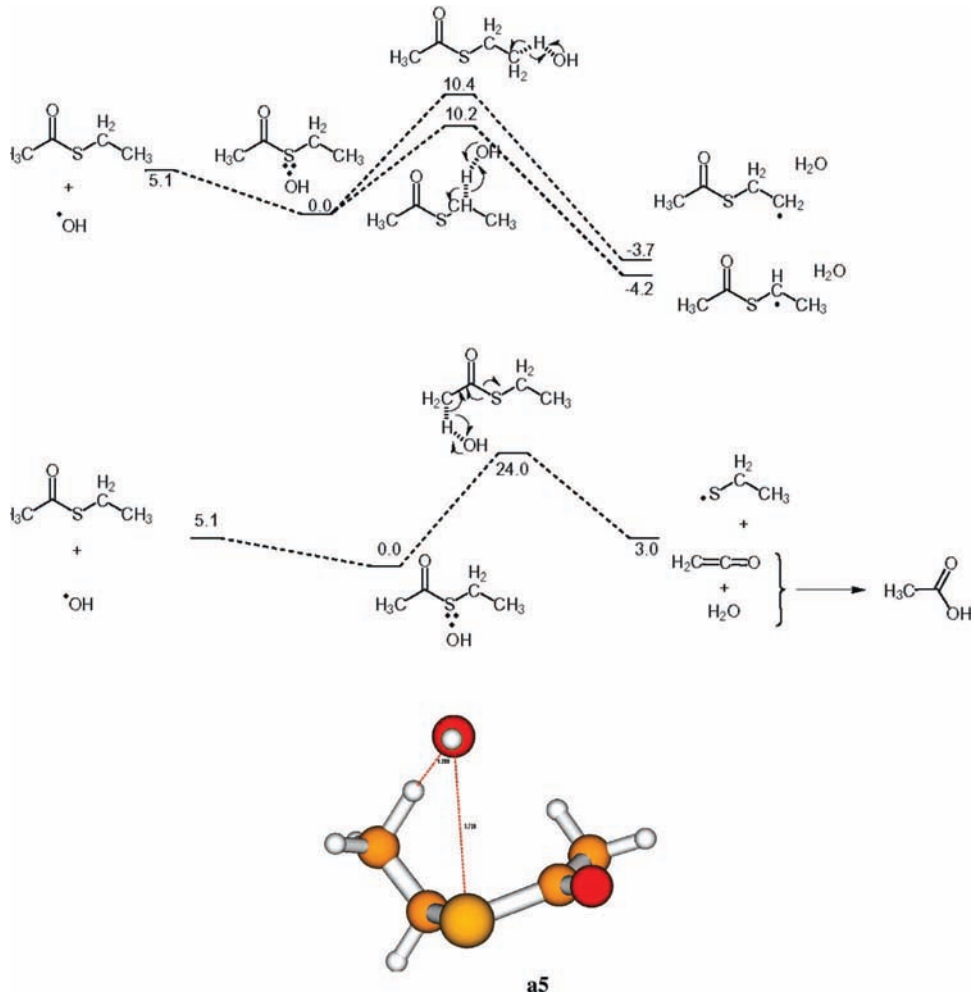

a5

Figure 5. Energy levels along the reaction pathway in SETAc. **a5** represents the structure of the transition state SETAc-TS1 with $E_a = 10.4$ kcal mol^{-1}.

10, 12, and 13). The BDE is lower by 13−19 kcal mol^{-1}. Similar to SETAc, the stability of all four C-centered radicals does not depend on the environment.

The reaction energies ($\Delta E'$) calculated in vacuum and in water indicate that the formation of the C-centered radicals via a direct H-atom abstraction by •OH radicals is strongly favorable, in particular, for the C-centered radical $H_3C-C(=O)-{}^{\bullet}CH-S-CH_2-CH_3$ $\Delta E' = -43.6$ kcal mol^{-1} in vacuum and $\Delta E' = -41.2$ kcal mol^{-1} in water (Table 4 entry 7). The formation of two other radicals, $H_2C^{\bullet}-C(=O)-CH_2-S-CH_2-CH_3$ and $H_3C-C(=O)-CH_2-S-{}^{\bullet}CH-CH_3$, is less energetically favorable ($\Delta E' = -16.1$ and -16.2 kcal mol^{-1} in vacuum, and $\Delta E' = -17.6$ and -17.8 kcal mol^{-1} in water, respectively; Table 4, entries 6 and 8). The formation of the fourth radical, $H_3C-C(=O)-CH_2-S-CH_2-{}^{\bullet}CH_2$, is even less favorable ($\Delta E' = -9.9$ kcal mol^{-1} in vacuum and $\Delta E' = -11.5$ kcal mol^{-1} in water; Table 4, entry 9). These values follow mostly the trend found for the BDEs.

Therefore, as far as the influence of the environment on the reaction energies ($\Delta E'$) is concerned, similar features were observed as for SETAc. The respective formation energies of C-centered radicals via a direct H-atom abstraction by •OH radicals are very similar in vacuum and in water (Table 4, entries 6−9).

Similar to what was found for SETAc, the reaction energies ($\Delta E''$) calculated in vacuum indicated that the formation of the C-centered radicals via deprotonation of the monomeric sulfur radical cation assisted by water is strongly unfavorable (Table 4, entries 6−9). Reaction energies ($\Delta E''$) calculated in water indicate that the formation of C-centered radicals via deprotonation of the respective monomeric radical cation is favorable, in particular, for the C-centered radical, $H_3C-C(=O)-{}^{\bullet}CH-S-CH_2-CH_3$ ($\Delta E'' = -19.9$ kcal mol^{-1}) (Table 4, entry 7). The formation of three other radicals, $H_2C^{\bullet}-C(=O)-CH_2-S-CH_2-CH_3$, $H_3C-C(=O)-CH_2-S-{}^{\bullet}CH-CH_3$, and $H_3C-C(=O)-CH_2-S-CH_2-{}^{\bullet}CH_2$ is less favorable energetically ($\Delta E' = -7.1$, -7.2, and -9.4 kcal mol^{-1}, respectively; Table 4, entries 6 and 8−9).

Contrary to what was found for SETAc, the formation of C-centered radicals via deprotonation of the monomeric sulfur radical cation assisted by water is less favorable than the formation via direct H-atom abstraction. For the most stable radical, $H_3C-C(=O)-{}^{\bullet}CH-S-CH_2-CH_3$, this difference is ∼21 kcal mol^{-1} (Table 4, entry 7).

Analogous to SETAc, the abstraction of hydrogen atoms from different carbon atoms was followed. For this purpose energies of the respective transition states (SETA-TS) were calculated (Table 5, entries 3−5). Contrary to SETAc, both the MP2 and B3LYP methods reveal the stability of the OH-adduct of SETA.

It was found that the activation energies for the formation of the three transition states SETA-TS1 (Figure 6, structure **b5**), SETA-TS2 (Figure 6, structure **b6**), and SETA-TS3 (Figure 6, structure **b7**) are in a quite broad range (of 5.6 to 11.1 kcal mol^{-1}) (Figure 6). The SETA-TS1 and SETA-TS2

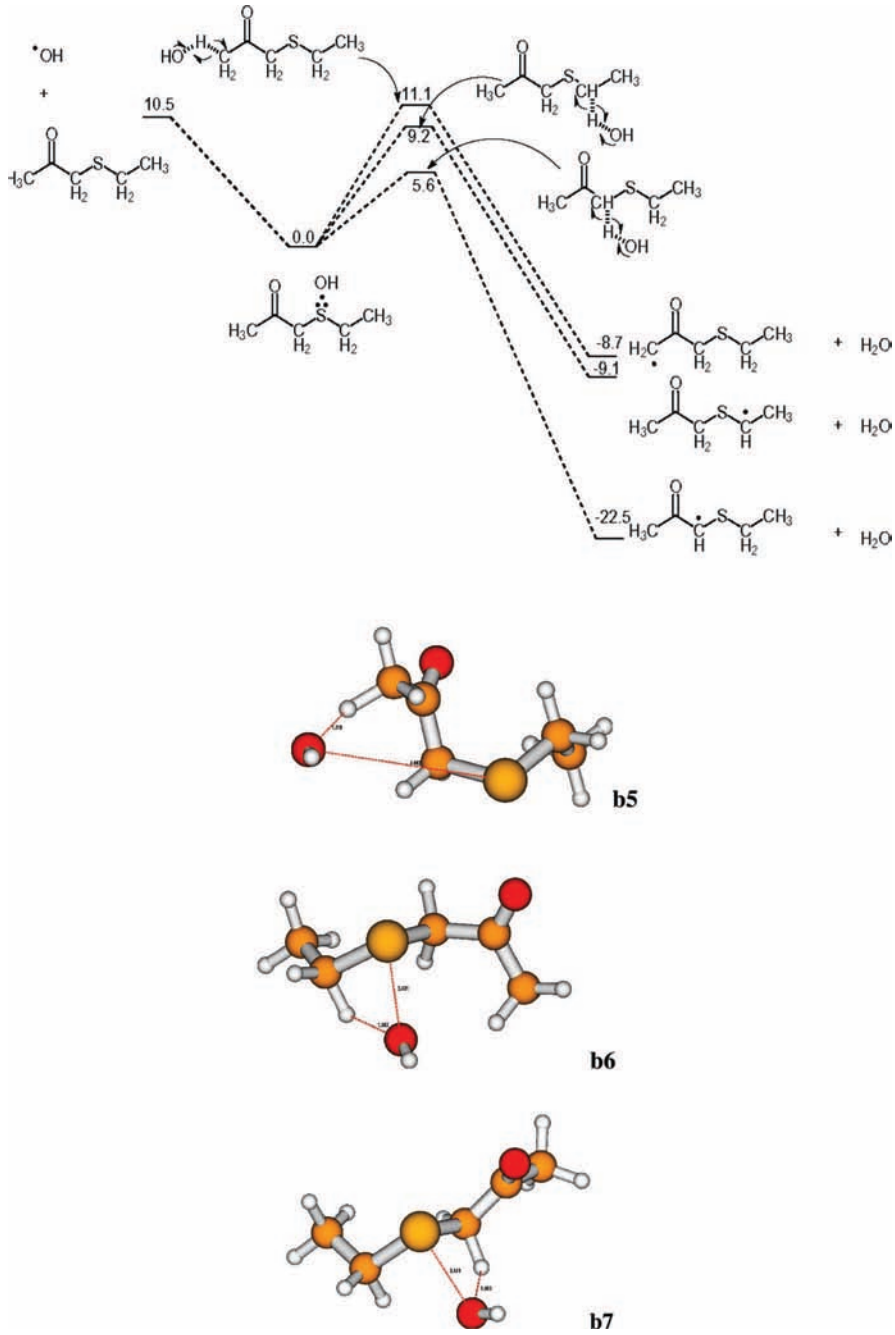

Figure 6. Energy levels along the reaction pathway in SETA. **b5** represents the structure of the transition state SETA-TS1 with $E_a = 11.1$ kcal mol^{-1}; **b6** represents the structure of the transition state SETA-TS2 with $E_a = 9.2$ kcal mol−1; **b7** represents the structure of the transition state SETA-TS3 with $E_a = 5.6$ kcal mol^{-1}.

convert into the two C-centered radicals with similar stabilization energies, −8.7 and −9.1 kcal mol^{-1}, respectively (Figure 6). The C-centered radical cation derived from SETA, $H_3C-C(=O)-{}^{\bullet}CH-S-CH_2-CH_3$, with the largest stabilization energy of −22.5 kcal mol^{-1} is also favored kinetically because of the lowest activation energy for the formation of the transition state SETA-TS3 which is equal to 5.6 kcal mol^{-1}. This is due to the captodative effect which stabilizes also the transition state.

Discussion

The present study aims to examine the influence of the mutual location of the carbonyl group and sulfur atom on the nature of transients which are formed during •OH-induced oxidation of SETAc and SETA.

Hydroxysulfuranyl Radicals. The primary transient resulting from the •OH radical attack on thioethers is the OH-adduct to the sulfur atom (hydroxysulfuranyl radical). Our electronic energy values obtained in vacuum for DMS are in agreement with the free energies obtained by McKee[8,42] (8.6 kcal/mol with our calculations versus 8.7 kcal/mol[42]). In water there is a discrepancy (1.8 kcal/mol with our calculations versus 3.0 kcal/mol[42]). However the magnitude of this discrepancy is within uncertainty connected with solvation energies.

Contrasting the structures of DMS and SETAc, in SETAc one methyl group of DMS is replaced by an acetyl group (a strongly electron withdrawing group). This substitution affects the electron density on the sulfur atom and has dramatic consequences as far as the stability of the hydroxysulfuranyl radical is concerned. The OH-adduct to the sulfur atom in

SETAc was found unstable using the MP2 method and with low stability using the B3LYP method, both in vacuum and in water (Table 2, entry 3). (Vide supra a comment on differences between MP2 and B3LYP results in the Computational methods section.) One has to note that calculations performed using the MP2 method are in agreement with the lack of experimental observation of the OH-adduct of SETAc in aqueous solutions.[27]

The very poor stability of the OH-adduct can be rationalized by its efficient direct conversion to the respective C-centered radicals. Two calculated transition states SETAc-TS1 and SETAc-TS2 (Figure 5) convert into the two C-centered radicals characterized by similar stabilization energies. The presence of C-centered radicals derived from SETAc was experimentally confirmed (vide infra in the subchapter C-centered radicals). Moreover, one of the calculated transition state SETAc-TS3 (the scenario when $^{\bullet}$OH radical approaches SETAc molecule from the acetyl group side) results in dissociation into acetic acid and ethylthiyl radical. Such reaction pathway for the OH-adduct of SETAc seems to be also confirmed experimentally since the formation of thiyl-type radicals was detected indirectly by the observation of a weak absorption spectrum with $\lambda_{max} = 540$ nm[27] characteristic for the thiylperoxyl radicals RSOO$^{\bullet}$.[49–51]However, the efficiency of this reaction pathway is minor, which is in line with a much higher calculated activation energy required to reach the transition state SETAc-TS3.

Different results for the OH-adduct were obtained in SETA. In the SETA molecule, contrary to the SETAc molecule, the acetyl group is not directly linked with the sulfur atom but is separated by one methylene group. Therefore, the electron-withdrawing character of the acetyl group is weakened. This fact has a significant effect on the stability of the OH-adduct in comparison to the analogous intermediate in SETAc. The OH-adduct in SETA was found to be stable in vacuum, however, unstable only by 1 kcal mol^{-1} in water (Table 2, entry 8). At this point, it should be noted that the formation of hydroxysulfuranyl radicals in SETA was detected directly in neutral aqueous solutions by the observation of an absorption spectrum with $\lambda_{max} = 340$ nm.[27] This fact points out that the MP2 method seems to underestimate the stability of the OH-adducts, especially in water (vide supra a comment in the Computational Methods section). In spite of the fact that the stability of the OH-adduct of SETA is lower than the stability of the OH-adduct of DMS, it has to be noted that the S−O bond is a 2c−3e bond characterized by a quasi-equal spin density distribution on the two atoms of the bond ($\rho_S/\rho_O = 0.55/0.60$)and their lengths in both adducts are similar, i.e. ∼2.07Å (Table 3, entries 1 and 11).

The poor stability of the OH-adduct in SETA can be rationalized in an analogous way as it was for the OH-adduct in SETAc, namely by its efficient direct conversion to the respective C-centered radicals. Formation of one of the three calculated transition states, i.e. SETA-TS3, is of particular interest since it has the lowest activation energy (Figure 6, structure **b7**) and it also converts to the C-centered radical with the highest stabilization energy (Figure 6). The presence of this C-centered radical was also experimentally confirmed (vide infra in the subchapter C-centered radicals).

Monomeric ($R_2S^{+\bullet}$) and Dimeric Sulfur Radical Cations ($RS\therefore SR_2)^+$. Formation of the monomeric radical cation in water was found unfavorable with and without the involvement of protons (Table 4, entry 1). However, contrary to the OH-adduct in SETAc, the monomeric radical cation derived from SETAc was found to be stable (Table 1, entry 8, and Table 3, entry 6). The calculated reaction energies for the formation of the monomeric radical cation are in contradiction to experimental observations where a very short-lived absorption in the range of $\lambda = 300-400$ nm was observed 90 ns after the electron pulse in N_2O- and O_2-saturated solutions at low pH.[27] This absorption was assigned to the monomeric radical cation from SETAc. Interestingly, formation of the dimeric radical cation from SMTAc and for SETAc were found energetically favorable (Table 2, entry 4). However, its formation was not experimentally observed. All of the facts mentioned above and taken together may suggest another very efficient reaction pathway responsible for the poor stability of the monomeric radical cation of SETAc. The reaction which has to be taken into consideration is deprotonation of the monomeric radical cation leading to the respective C-centered radicals (vide infra in the C-centered chapter).

Important information concerning properties of the monomeric sulfur radical cation of SETA can be deduced from the observed efficient formation of the $H_3C-C(=O)-^{\bullet}CH-S-CH_2-CH_3$ radicals under low and neutral pH conditions. The experimental results at low (<5 mM) and high (25 mM) concentration of SETA, at neutral pH, clearly indicate that the decay of the hydroxysulfuranyl radical does not lead to the formation of the dimeric radical cations of SETA but to the C-centered radical $H_3C-C(=O)-^{\bullet}CH-S-CH_2-CH_3$ instead.[27] This observation is in line with the calculated unfavorable formation of the monomeric sulfur radical cations of SETA where protons are not involved (Table 4, entry 5 for $\Delta E'$). On the other hand, formation of the $H_3C-C(=O)-^{\bullet}CH-S-CH_2-CH_3$ radical *via* direct hydrogen abstraction is energetically and kinetically highly favorable (vide infra in the C-centered radicals chapter).

A somewhat different picture was observed experimentally at low pH. At low concentration of SETA (<5 mM) formation of the dimeric radical cations was again not efficient. On the other hand, when the concentration of SETA was increased to 25 mM, efficient formation of the dimeric radical cations was observed.[27] This last observation is in agreement with the energetically favorable formation of the monomeric sulfur radical cations of SETA where protons are involved (Table 4, entry 5 for $\Delta E''$). It is also in agreement with the stabilization of the dimeric radical cations of SETA (Table 2 entry 9). The low efficiency of the dimeric radical cations at low concentration of SETA is likely due to the efficient deprotonation of the monomeric sulfur radical cations to the $H_3C-C(=O)-^{\bullet}CH-S-CH_2-CH_3$ radicals. Reaction energy calculated in water indicated that formation of the $H_3C-C(=O)-^{\bullet}CH-S-CH_2-CH_3$ radical is energetically favorable by 19.9 kcal mol^{-1} (Table 4, entry 7 for $\Delta E''$).

C-Centered Radicals. Three different C-centered radicals can be formed in SETAc since the calculated reaction energies indicated that their formations via two reaction pathways (direct hydrogen abstraction and/or deprotonation of the monomeric radical cation) are energetically favorable in water. Experimental results, at low and neutral pH, show the formation of an absorption spectrum with two absorption maxima at $\lambda_{max} = 280$ and 420 nm.[27] The C-centered radical $H_3C-^{\bullet}CH-S-C(=O)CH_3$ is likely responsible for that absorption. This radical is slightly more stable than the C-centered radicals $H_2C^{\bullet}-CH_2-S-^{\bullet}C(=O)-CH_3$ and $H_2C^{\bullet}-C(=O)-S-CH_2-CH_3$ (Table 4, entries 2−4). Moreover, this radical is favored kinetically since the activation energy required for reaching the transition state SETAc-TS2 is the lowest calculated (Figure 5). The experimental data indicate

the presence of the second C-centered radical with a weak absorption within the range of $\lambda = 300-350$ nm.[27] Considering the energies of formation (Table 4, entries 2 and 4) and the bond dissociation energies (Table 2, entries5 and 7) of the C-centered radicals derived from SETAc, the $H_2C^{\bullet}-C(=O)-S-CH_2-CH_3$ radical might be responsible for this absorption.

In SETA, formation of four different C-centered radicals is possible since the calculated reaction energies indicated that their formations via two reaction pathways are energetically favorable in water. Of significance, the formation of the one of the C-centered radicals is energetically and kinetically highly favorable. The good stability of the C-centered radical $H_3C-C(=O)-{}^{\bullet}CH-S-CH_2-CH_3$ ensues from the captodative effect since the radical site is located between an electron-donating sulfur atom and an electron-withdrawing acetyl group.

Considering the energies of formation of the C-centered radicals (Table 4, entries 6−9) and the bond dissociation energies (Table 2, entries 10−13) derived from SETA, the formation of $H_3C-C(=O)-{}^{\bullet}CH-S-CH_2-CH_3$ radical via direct hydrogen abstraction or deprotonation of the respective monomeric radical cation is favorable by ∼23.5 and by ∼12.8 kcal mol^{-1}, respectively, as compared to the next two most stable radicals $H_2C^{\bullet}-C(=O)-CH_2-S-CH_2-CH_3$, $H_3C-C(=O)-CH_2-S-{}^{\bullet}CH-CH_3$.

Considering the activation energies required for the formation of the respective transition states in SETA (Figure 6), one should note that the activation energy of the transition state SETA-TS3 (**b7**) is lower by nearly 3.6 and 5.5 kcal mol^{-1} compared to the transition states SETA-TS2 (**b6**) and SETA-TS1 (**b5**), respectively.

These calculated results have a strong impact on the interpretation of the experimental results obtained in aqueous solutions containing SETA. The experimental results indicate the formation of an absorption spectrum with two absorption maxima at $\lambda_{max} = 290$ and 380 nm.[27] This spectrum was observed in the following conditions: (i) immediately after the pulse, at low pH and low SETA concentration; (ii) after decay of the dimeric sulfur radical cations, at low pH and at very high SETA concentration (>5 mM); (iii) after decay of the hydroxysulfuranyl radical, at neutral pH, both at low and high concentrations of SETA. Taking into account the $^{\bullet}OH$-induced oxidation mechanism described by reactions 1−7 (vide Introduction) this absorption spectrum has to be assigned to the C-centered radicals, and $H_3C-C(=O)-{}^{\bullet}CH-S-CH_2-CH_3$ radical is now with no doubts the only reasonable candidate.

Conclusions

The new results of ab initio and DFT calculations obtained for SETAc and SETA provided assistance for us to interpretate our pulse radiolysis experimental data[27] and thus better support for the proposed $^{\bullet}OH$-induced reaction mechanism. In most of the cases a consistent picture was obtained between the calculations and the experiment.

In accord with the experiment, it was found that the α-positioned acetyl group in S-ethylthioacetate (SETAc) destabilizes its hydroxysulfuranyl radicals and its monomeric sulfur radical cations. Accordingly, formation of the stable C-centered radicals of the α-(alkylthio)alkyl-type was found to be energetically favorable. The $H_3C-{}^{\bullet}CH-S-C(=O)CH_3$ radical, in particular, was found energetically and kinetically most favorable and responsible for the absorption spectrum with two absorption maxima at $\lambda_{max} = 280$ and 420 nm observed in pulse radiolysis experiments.

On the other hand, in accordance with experiment, the β-positioned acetyl group in *S*-ethylthioacetone (SETA) does not destabilize hydroxysulfuranyl radicals, monomeric sulfur radical cations, and the dimeric sulfur radical cations. Moreover, the α-(alkylthio)alkyl radicals of the type $-S-{}^{\bullet}CH-C(=O)-$ were found to be particularly stabilized and their formation was kinetically favored because of the respective transition state formed with the lowest activation energy.

From the mechanistic point of view, it is important to note that the low activation energies of the transition states found on the reaction pathways accounting for the efficient direct conversion of the hydroxysulfuranyl radicals of SETAC and SETA into their respective C-centered radicals. This reaction pathway, important in neutral solutions, is responsible for the absence of dimeric radical cations of SETAc at low and high concentrations and of dimeric radical cations of SETA at relatively low concentrations.

Acknowledgment. The computation was performed employing the computing resources of the Institut de Développement et des Ressources en Informatique Scientifique (IDRIS) for computer time (project 060946) and the Centre de Calcul Recherche (CCR-Université Paris 6, Paris, France). The authors are indebted to Dr. Gordon L. Hug and to Prof. Chantal Houée-Levin for their helpful comments during careful reading the manuscript.

References and Notes

(1) Asmus, K.-D.; Bonifačić, M. Sulfur-centered reactive intermediates as studied by radiation chemical and complementary techniques. In *S-Centered Radicals*; Alfassi, Z. B., Ed.; John Wiley & Sons Ltd.: Chichester, 1999; pp 141−191.

(2) Asmus, K.-D. Sulfur-centered three-electron bonded radical species. In *Sulfur-Centered Reactive Intermediates in Chemistry and Biology*; Chatgilialoglu, C., Asmus K.-D., Eds.; Plenum Press: New York, 1990; pp 155−172.

(3) Asmus, K.-D.; Bahnemann, D.; Bonifačić, M.; Gillis, H. A. *Faraday Discuss. Chem. Soc.* **1978**, *63*, 213–225.

(4) Bonifačić, M.; Möckel, H.; Bahnemann, D.; Asmus, K.-D. *J. Chem. Soc., Perkin Trans. 2* **1975**, 675–685.

(5) Bahnemann, D.; Asmus, K.-D. *J. Chem. Soc. Chem. Commun.* **1975**, 238.

(6) Bobrowski, K.; Hug, G. L.; Pogocki, D.; Marciniak, B.; Schöneich, C. C. *J. Phys. Chem. B* **2007**, *111*, 9608–9620.

(7) Bobrowski, K.; Hug, G. L.; Pogocki, D.; Marciniak, B.; Schöneich, C. *J. Am. Chem. Soc.* **2007**, *129*, 9236–9246.

(8) Mishra, B.; Priyadarsini, K. I.; Mohan, H. H. *Res. Chem. Intermed.* **2005**, *31*, 625–632.

(9) Mohan, H.; Mittal, J. P. *Radiat. Phys. Chem.* **2005**, *74*, 220–226.

(10) Schöneich, C.; Pogocki, D.; Hug, G. L.; Bobrowski, K. *J. Am. Chem. Soc.* **2003**, *125*, 13700–13713.

(11) Varmenot, N.; Remita, S.; Abedinzadeh, Z.; Wisniowski, P.; Strzelczak, G.; Bobrowski, K. *J. Phys. Chem. A* **2001**, *105*, 6867–6875.

(12) Asmus, K.-D. Heteroatom-centered free radicals. Some selected contributions by radiation chemistry. In *Radiation Chemistry: Present Status and Future Prospects*; Jonah, C., Rao B. S. M., Eds.; Elsevier Science: Amsterdam, 2001; pp 341−393.

(13) Schöneich, C.; Pogocki, D. D.; Wisniowski, P.; Hug, G. L.; Bobrowski, K. *J. Am. Chem. Soc.* **2000**, *122*, 10224–10225.

(14) Bobrowski, K.; Hug, G. L.; Marciniak, B.; Schöneich, C.; Wiśniowski, P. *Res. Chem. Intermed.* **1999**, *25*, 285–297.

(15) Gawandi, V. B.; Mohan, H.; Mittal, J. P. *J. Chem. Soc. Perkin Trans. 2* **1999**, 1425–1432.

(16) Bobrowski, K.; Pogocki, D.; Schöneich, C. *J. Phys. Chem. A* **1998**, *102*, 10512–10521.

(17) Bobrowski, K.; Hug, G. L.; Marciniak, B.; Miller, B. L.; Schöneich, C. *J. Am. Chem. Soc.* **1997**, *119*, 8000–8011.

(18) Schöneich, C.; Bobrowski, K. *J. Am. Chem. Soc.* **1993**, *115*, 6538–6547.

(19) Bobrowski, K.; Pogocki, D.; Schöneich, C. *J. Phys. Chem.* **1993**, *97*, 13677–13684.

(20) Bobrowski, K.; Schöneich, C. *J. Chem. Soc., Chem. Commun.* **1993**, 795–797.

(21) Steffen, L. K.; Glass, R. S.; Sabahi, M.; Wilson, G. S.; Schöneich, C.; Mahling, S.; Asmus, K.-D. *J. Am. Chem. Soc.* **1991**, *113*, 2141–2145.

(22) Asmus, K.-D.; Göbl, M.; Hiller, K.-O.; Mahling, S.; Mönig, J. *J. Chem. Soc., Perkin Trans. 2* **1985**, 641–646.
(23) Glass, R. S.; Hojjatie, M.; Wilson, G. S.; Mahling, S.; Göbl, M.; Asmus, K.-D. *J. Am. Chem. Soc.* **1984**, *106*, 5382–5383.
(24) Hiller, K.-O.; Masloch, B.; Göbl, M.; Asmus, K.-D. *J. Am. Chem. Soc.* **1981**, *103*, 2734–2743.
(25) Asmus, K.-D. *Nukleonika* **2000**, *45*, 3–10.
(26) Glass, R. S. Neighboring group participation: general principles and application to sulfur-centered reactive species. In *Sulfur-Centered Reactive Intermediates in Chemistry and Biology*; Chatgilialoglu, C., Asmus, K.-D., Eds.; Plenum Press: New York, 1990; Vol. 197, pp 213−226.
(27) Varmenot, N.; Bergès, J.; Abedinzadeh, Z.; Scemama, A.; Strzelczak, G.; Bobrowski, K. *J. Phys. Chem. A* **2004**, *108*, 6331–6346.
(28) Frisch, M. J.; Trucks, G. W.; Schlegel, H. B.; Scuseria, G. E.; Robb, M. A.; Cheeseman, J. R.; Zakrzewski, V. G.; Montgomery, J. J. A.; Stratmann, R.; Burant, J. C.; Dapprich, S.; Millam, J. M.; Daniels, A. D.; Kudin, K. N.; Strain, M. C.; Farkas, O.; Tomasi, J.; Barone, V.; Cossi, M.; Cammi, R.; Mennucci, B.; Pomelli, C.; Adamo, C.; Clifford, S.; Ochterski, J.; Petersson, G. A.; Ayala, P. Y.; Cui, Q.; Morokuma, K.; Malick, D. K.; Rabuck, A. D.; Raghavachari, K.; Cioslowski, J. Ortiz, J. V.; Baboul, A. G.; Stefanov, B. B.; Liu, G.; Liashenko, A.; Piskorz, P.; Komoromi, I.; Gomperts, R.; Martin, R. L.; Fox, D. J.; Keith, T.; Al-Laham, M. A.; PJ.; C. Y. eng, Nanayakkara, A.; Gonzalez, C.; Challacombe, M.; Gill, P. M. W.; Johnson, B.; Chen, W.; Wong, M. W.; Andres, J. L.; Head-Gordon, M.; Replogle, E. S.; Pople, J. A. *Gaussian 98*, revision A.7; Gaussian Inc: Pittsburgh, PA, 1998.
(29) Frisch, M. J.; Trucks, G. W.; Schlegel, H. B.; Scuseria, G. E.; Robb, M. A.; Cheesemann, J. R.; Montgomery, J. J. A.; Vreven, T.; Kudin, K. N.; Burant, J. C.; Millam, J. M.; Iyengar, S. S.; Tomasi, J.; Barone, V.; Mennuci, B.; Cossi, M.; Scalmani, G.; Rega, N.; Petersson, G. A.; Nakatsuji, H.; Hada, M.; Ehara, M.; Toyota, K.; Fukuda, R.; Hasegawa, R. J.; Ishida, M.; Nakajima, T.; Honda, Y.; Kitao, O.; Nakai, H.; Klene, M.; Li, X.; Knox, J. E.; Hratchian, H. P.; Cross, J. B.; Adamo, C.; Jaramillo, J.; Gomperts, J. R.; Stratmann, R. E.; Yazyev, O.; Austin, A. J.; Cammi, A. R.; Pomelli, C.; Ochterski, J.; Ayala, P. Y.; Morokuma, K.; Voth, G. A.; Salvador, P.; Dannenberg, J. J.; Zakrzewski, V. G.; Dapprich, S.; Daniels, A. D.; Strain, M. C.; Farkas, O.; Malick, D. K.; Rabuck, A. D.; Raghavachari, K.; Foresman, J. B.; Ortiz, J. V.; Cui, Q.; Baboul, A. G.; Clifford, S.; Cioslowski, J.; Stefanov, B. B.; Liu, G.; Liashenko, A.; Piskorz, P.; Komaromi, I.; Martin, R. L.; Fox, D. J.; Keith, T.; Al-Laham, M. A.; Peng, C. Y.; Nanayakkara, A. M. C.; Gill, P. M.; Johnson, B.; Chen, W.; Wong, M. W.; Gonzalez, C.; Pople, A. J. *Gausian 03*, revision B.03; Gaussian Inc.: Pittsburgh PA, 2003.
(30) Li, X.; Cai, Z.; Sevilla, M. D. *J. Phys. Chem. A* **2002**, *106*, 1596–1603.
(31) Rauk, A.; Armstrong, D. A.; Bergès, J. *Can. J. Chem.* **2001**, *79*, 405–417.
(32) Fourré, I.; Silvi, B. *Heteroatom Chem.* **2007**, *18*, 135–160.
(33) Brunelle, P.; Schöneich, C.; Rauk, A. *Can. J. Chem.* **2006**, *84*, 893–904.
(34) Fourré, I. I.; Bergès; J., *J. Phys. Chem. A* **2004**, *108*, 898–906.
(35) Carmichael, I. *Nukleonika* **2000**, *45*, 11–17.
(36) Braïda, B.; Hiberty, P. C. *J. Phys. Chem. A* **2000**, *104*, 4618–4628.
(37) Braïda, B.; Hiberty, P. C.; Savin, A. J. *J. Phys. Chem. A* **1998**, *102*, 7872–7877.
(38) Uchimaru, T.; Tsuzuki, S.; Sugie, M.; Tokuhashi, K.; Sekiya, A. *Chem. Phys. Lett.* **2005**, *408*, 216–220.
(39) McKee, M. L. *J. Phys. Chem.* **1993**, *97*, 10971–10976.
(40) Cossi, M. M.; Adamo, C.; Barone, V. *Chem. Phys. Lett.* **1998**, *297*, 1–7.
(41) Cossi, M.; Barone, V.; Mennucci, B.; Tomasi, J. *Chem. Phys. Lett.* **1998**, *286*, 253–260.
(42) McKee, M. L. *J. Phys. Chem. A* **2003**, *107*, 6819–6827.
(43) Zhan, C.-G.; Dixon, D. A. *J. Phys. Chem. A* **2002**, *106*, 9737–9744.
(44) Williams, M. B.; Campuzano-Jost, P.; Cossairt, B. M.; Hynes, A. J.; Pounds, A. J. *J. Phys. Chem. A* **2007**, *111*, 89–104.
(45) Gross, A.; Barnes, I.; Sørensen, R. M.; Kungsted, J.; Mikkelsen, K. V. *J. Phys. Chem. A* **2004**, *108*, 8659–8671.
(46) Maity, D. K. *J. Am. Chem. Soc.* **2002**, *124*, 8321–8328.
(47) Wang, L.; Zhang, J. *J. Mol. Struct.* **2001**, *543*, 167–1??
(48) Tureček, F. *J. Phys. Chem.* **1994**, *98*, 3701–3706.
(49) Zhang, X.; Zgang, N.; Schuchmann, H.-P.; von Sonntag, C. *J. Phys. Chem.* **1994**, *98*, 6541–6547.
(50) Tamba, M.; Simone, G.; Quintilani, M. *Int. J. Radiat. Biol.* **1986**, *50*, 595–600.
(51) Jayson, G. G.; Stirling, D. A.; Swallow, A. J. *Int. J. Radiat. Biol.* **1971**, *19*, 143–156.

JP711944V